Inorg. Chem. **2003**, *42*, 1734–1738

$Mn_{\sim 2.4}Mo_6O_9$: First Example of Empty Twin Chains of Edge-Sharing M_6 Octahedra in Transition Metal Cluster Chemistry

Nicolas Barrier and Patrick Gougeon*

Université de Rennes I, Institut de Chimie, Laboratoire de Chimie du Solide et Inorganique Moléculaire, U.M.R. no. 6511, Avenue du Général Leclerc, 35042 Rennes Cedex, France

Richard Retoux and Henri Leligny

Laboratoire CRISMAT, UMR 6508, ISMRA et Université de Caen, 6, Boulevard du Maréchal Juin, 14050 Caen Cedex, France

Received September 16, 2002

The novel ternary reduced molybdenum oxide $Mn_{\sim 2.4}Mo_6O_9$ has been synthesized by solid-state reaction at 1400 °C for 96 h in sealed molybdenum crucibles. Electron diffraction studies showed that $Mn_{\sim 2.4}Mo_6O_9$ presents a complex crystal structure with a 3d incommensurate modulation. The average crystal structure was determined on a single-crystal by X-ray diffraction in the orthorhombic space group *Pnma* with the following lattice parameters: $a = 16.4824(2)$ Å, $b = 2.8273(2)$ Å, $c = 17.3283(2)$ Å, $Z = 4$. The Mo network consists of empty twin chains of trans-edge-sharing octahedra that occur for the first time in a solid-state compound. The Mo–Mo distances within the chains range from 2.62 to 2.92 Å, and the Mo–O distances from 1.99 to 2.17 Å as usually observed in the reduced molybdenum oxides. Single-crystal resistivity measurements show that $Mn_{\sim 2.4}Mo_6O_9$ is metallic between 4.2 and 300 K. The magnetic susceptibility data indicate paramagnetic behavior due to the Mn^{2+} moment at high temperatures with a weak ferromagnetic behavior below 80 K.

Introduction

The structural chemistry of compounds containing reduced molybdenum has grown tremendously over the last two decades so that 22 different types of discrete molybdenum clusters, of which the nuclearities goes from 3 to 36, are known to date.[1] Clusters with nuclearities higher than 8 result generally from the one-dimensional condensation of Mo_6 clusters via opposite face- or edge-sharing depending on the ligand environment. The former process is observed when the Mo_6 clusters are face-bridged by the ligands (S, Se, and Te) and is well exemplified by the series of compounds $M_{2n-2}Mo_{6n}X_{6n+2}$ (M = Rb, Cs; X = S, Se, Te).[2] The second one is encountered in the reduced molybdenum oxides where the Mo_6 clusters are edge-bridged by the oxygens and occurs in the series $M_{n-x}Mo_{4n+2}O_{6n+4}$[3] ($n = 2$, $x = 0$ for M = Ca, Sr, Sn, Pb, La−Gd; $n = 3$, $x = 0$ for M = K; $n = 4$ and 5, $x = 1$ for M = Ba, and $x = -1$ for M = In). The ultimate step of these one-dimensional condensations is the formation of infinite chains of formula $|Mo_{6/2}|^1_\infty$ for the face-sharing condensation process and $|Mo_2Mo_{4/2}|^1_\infty$ for the edge-sharing one. The former type of chain is found in the quasi-one-dimensional compounds $M_2Mo_6X_6$ (M = Na, K, Rb, Cs; X = S, Se, or Te)[4] and the latter one in the different four

* To whom correspondence should be addressed. E-mail: Patrick.Gougeon@univ-rennes1.fr.

(1) (a) Simon A. *Angew. Chem., Int. Ed. Engl.* **1988**, *27*, 159−185. (b) Simon A. In *Clusters and Colloids*; Schmid, G., Ed.; VCH: Weinheim, 1994, pp 373−458.

(2) (a) Gougeon, P.; Potel, M.; Padiou, J.; Sergent, M. *Mater. Res. Bull.* **1987**, *22*, 1087−1093. (b) Gougeon, P.; Potel, M.; Padiou, J.; Sergent, M. *Mater. Res. Bull.* **1988**, *23*, 453−460. (c) Thomas, C.; Picard, S.; Gautier, R.; Gougeon, P.; Potel, M. *J. Alloys Compd.* **1997**, *262*−*263*, 305−310. (d) Picard, S.; Gougeon, P.; Potel, M. *Angew. Chem., Int. Ed.* **1999**, *38*, 2034−2036.

(3) (a) Hibble, S. J.; Cheetham, A. K.; Bogle, A. R. L.; Wakerley, H. R.; Cox, D. E. *J. Am. Chem. Soc.* **1988**, *110*, 3295. (b) Dronskowski, R.; Simon, A. *Angew. Chem., Int. Ed. Engl.* **1989**, *28*, 758. (c) Gougeon, P.; Potel, M.; Sergent, M. *Acta Crystallogr.* **1990**, *C46*, 1188. (d) Gougeon, P.; Gall, P.; Sergent, M. *Acta Crystallogr.* **1991**, *C47*, 421. (e) Dronskowski, R.; Simon, A.; Mertin, W. *Z. Anorg. Allg. Chem.* **1991**, *602*, 49. (f) Gall, P.; Gougeon, P. *Acta Crystallogr.* **1994**, *C50*, 7. (g) Gall, P.; Gougeon, P. *Acta Crystallogr.* **1994**, *C50*, 1183. (h) Dronskowski, R.; Simon, A.; Mertin. W. *Z. Anorg. Allg. Chem.* **1991**, *602*, 49. (i) Dronskowski, R.; Simon, A. *Acta Chem. Scand.* **1991**, *45*, 850. (j) Schimek, G. L.; Chen, S. C.; McCarley, R. E. *Inorg. Chem.* **1995**, *34*, 6130. (k) Schimek, G. L.; Nagaki, D. A.; McCarley, R. E. *Inorg. Chem.* **1994**, *33*, 1259. (l) Dronskowski, R.; Mattausch, H. J.; Simon, A. *Z. Anorg. Allg. Chem.* **1993**, *619*, 1397. (m) Schimek, G. L.; McCarley, R. E. *J. Solid State Chem.* **1994**, *113*, 345.

(4) Potel, M.; Chevrel, R.; Sergent, M. *Acta Crystallogr.* **1980**, *B36*, 1319.

10.1021/ic0260365 CCC: $25.00
Published on Web 02/08/2003

structure types $NaMo_4O_6$,[5] $Sc_{0.75}Zn_{1.25}Mo_4O_7$,[6] MMo_8O_{11},[7] $Mn_{1.5}Mo_8O_{11}$,[8] and $Ho_4Mo_4O_{11}$.[9] We present here the synthesis, structure, and properties of an original reduced molybdenum oxide, $Mn_{\sim 2.4}Mo_6O_9$, which constitutes a further step in the Mo_6 cluster condensation owing to the coupling of two Mo_4O_6-type chains. This new oxomolybdate is also to our knowledge the first noncubic compound presenting a three-dimensional incommensurate modulation.

Experimental Section

Synthesis. $Mn_{\sim 2.4}Mo_6O_9$ was first obtained as single-crystals in an attempt to synthesize a phase $LaMn_xMo_{8-y}O_{14}$ isostructural with $EuV_xMo_{8-y}O_{14}$.[10] The stoichiometry was only known after a complete structural study on a single-crystal by X-ray diffraction. Subsequently, single-phase powder of $Mn_{\sim 2.4}Mo_6O_9$ was obtained by high-temperature solid-state reaction from the required stoichiometric mixture of MoO_3, MnO_2, and Mo. Theses powders were mixed, ground together in a mortar, and then cold-pressed using a hand press. The pellet was then loaded in a molybdenum crucible, which was sealed under a low argon pressure using an arc welding system. The crucible was heated at a rate of 300 K h^{-1} to 1673 K and held there for 4 days, then cooled at 100 K h^{-1} to 1300 K, and finally furnace cooled to room temperature. Attempts to synthesize compounds with different compositions in manganese (i.e., $Mn_{2.25}Mo_6O_9$, $Mn_{2.35}Mo_6O_9$, and $Mn_{2.5}Mo_6O_9$) were unsuccessful and have led to multiphasic samples with $Mn_{1.5}Mo_8O_{11}$[11] and $Mn_2Mo_3O_8$[12] as main impureties. The quasiabsence of nonstoichiometry in manganese was also confirmed by the X-ray studies made on single-crystals coming from the last three preparations. Indeed, after refinement of the site occupancy factors of the manganese ions, the calculated stoichiometries were $Mn_{2.44(4)}Mo_6O_9$, $Mn_{2.43(4)}Mo_6O_9$, and $Mn_{2.44(3)}Mo_6O_9$, respectively.

Single-Crystal Structure Determinations. A black needlelike crystal of approximate dimensions $0.28 \times 0.028 \times 0.027$ mm^3 was selected for data collection. Intensity data were collected on a Nonius Kappa CCD diffractometer using graphite-monochromatized Mo Kα radiation ($\lambda = 0.71073$ Å) at room temperature. The frames were recorded using $\Delta\omega = 2°$ rotation scans with an X-ray exposure time of 60 s. Reflection indexing, Lorentz-polarization correction, peak integration, and background determination were performed using the program DENZO of the Kappa CCD software package.[13] An empirical absorption correction was applied with the SORTAV program[14] ($T_{min} = 0.3917$, $T_{max} = 0.5330$). Analysis of the data revealed that the systematic absences (0*kl*) $k + l = 2n + 1$ and (*hk*0) $h = 2n + 1$ were consistent with the orthorhombic space group *Pnma*. Of 19781 reflections collected in the 1−37.78° θ range, 2486 were independent ($R_{int} = 0.0562$). The structure was solved by direct methods using SHELXS[15] and subsequent difference Fourier syntheses. All structure refinements and Fourier syntheses were carried out using SHELXL-97.[15] The positional and anisotropic displacement parameters for all atoms as well as the occupancy factors for the Mn atoms were refined to the values R1 = 0.0344, wR2 = 0.0763 for 127 parameters and 2244 reflections with $I > 2\,\sigma(I)$, and the residual electron densities were 2.695 and −2.818 e Å^{-3}. A summary of the X-ray crystallographic and experimental data is presented in Table 1. Atomic coordinates and equivalent isotropic displacement parameters, and selected interatomic distances, are reported in Tables 2 and 3, respectively.

Table 1. X-ray Crystallographic and Experimental Data for $Mn_{\sim 2.4}Mo_6O_9$

formula	$Mn_{2.44}Mo_6O_9$
fw, g mol^{-1}	853.69
space group	*Pnma*
a, Å	16.4824(2)
b, Å	2.8273(2)
c, Å	17.3283(2)
V, Å^3	807.51(6)
Z	4
ρ_{calcd}, g cm^{-3}	7.022
T, °C	20
λ, Å	0.71073 (Mo Kα)
μ, cm^{-1}	127.11
R1[a] (on all data)	0.0344
wR2[b] (on all data)	0.0763

[a] $R1 = \sum||F_o| - |F_c||/\sum|F_o|$. [b] $wR2 = \{\sum[w(F_o^2 - F_c^2)^2]/\sum[w(F_o^2)^2]\}^{1/2}$, $w = 1/[\sigma^2(F_o^2) + (0.00124P)^2 + 18.1011P]$ where $P = [\max(F_o^2,0) + 2F_c^2]/3$.

Table 2. Atomic Coordinates ($\times 10^4$), Site Occupancy Factors, and Equivalent Isotropic Displacement Parameters (Å^2 $\times$ 10^3) for $Mn_{\sim 2.4}Mo_6O_9$[a]

	SOF	*x*	*y*	*z*	*U*(eq)
Mo(1)	1	4632(1)	2500	6273(1)	5(1)
Mo(2)	1	689(1)	−2500	9704(1)	5(1)
Mo(3)	1	1701(1)	2500	10714(1)	10(1)
Mo(4)	1	3839(1)	−2500	10785(1)	5(1)
Mo(5)	1	4470(1)	2500	9505(1)	5(1)
Mo(6)	1	5098(1)	−2500	8266(1)	9(1)
Mn(1)	0.704(7)	1476(1)	−2500	7932(1)	35(1)
Mn(2)	0.288(8)	2264(3)	−2500	7181(3)	64(4)
Mn(3)	0.708(7)	3329(1)	−2500	7644(1)	35(1)
Mn(4)	0.289(7)	2622(3)	−2500	8834(2)	41(2)
Mn(5)	0.451(6)	2639(1)	2500	9198(1)	21(1)
O(1)	1	993(3)	2500	6982(2)	9(1)
O(2)	1	1922(3)	−2500	9867(3)	9(1)
O(3)	1	4182(3)	2500	8346(2)	9(1)
O(4)	1	4796(3)	−2500	7107(2)	11(1)
O(5)	1	5873(3)	2500	6160(2)	8(1)
O(6)	1	2950(2)	2500	10958(3)	8(1)
O(7)	1	3419(3)	2500	6595(3)	9(1)
O(8)	1	3561(2)	−2500	9627(2)	6(1)
O(9)	1	2436(3)	2500	8033(4)	51(3)

[a] *U*(eq) is defined as one-third of the trace of the orthogonalized U_{ij} tensor.

Transmission Electron Microscopy Studies. The high-resolution electron microscopy (HREM) and electron diffraction (ED) studies were performed on a 200 KV side entry JEOL 2010 electron microscope (tilt ±30°). Thin crystals were crushed in an agate mortar and suspended in alcohol, and a few droplets of the suspension were put on a carbon coated holey film to prepare the specimen for electron microscopy.

Electrical Resistivity Measurements. The ac resistivity was measured on single-crystals at 80 Hz with a current amplitude of

(5) (a) Torardi, C. C.; McCarley, R. E. *J. Am. Chem. Soc*. **1979**, *101*, 3963. (b) McCarley, R. E. *Polyhedron* **1986**, *5*, 51.
(6) (a) McCarley, R. E. *ACS Symp. Ser*. **1981** *155*, 41. (b) McCarley, R. E. *Philos. Trans. R. Soc. London, Ser. A* **1982**, *308*, 41.
(7) Lii, K. H.; McCarley, R. E..; Kim, S.; Jacobson, R. A. *J. Solid State Chem*. **1986**, *64*, 347.
(8) McCarley, R. E.; Lii, K. H.; Edwards, P. A.; Brough, L. F. *J. Solid State Chem*. **1985**, *57*, 17.
(9) Gougeon, P.; Gall, P.; McCarley, R. E. *Acta Crystallogr*. **1991**, *C47*, 1585.
(10) Leligny, H.; Grebille, D.; Roussel, P.; Labbé, Ph.; Hervieu, M.; Raveau, B.; Tortelier, J.; Gougeon, P. *Acta* Crystallogr. **1999**, *B*55, 467−483.
(11) Carlson, C. D.; Brough, L. F.; Edwards, P. A.; McCarley, R. E. *J. Less-Common Met*. **1989**, *156*, 325.
(12) Bertrand, D.; Kerner-Czeskleba, H. *J. Phys*. **1975**, 379.
(13) *COLLECT: KappaCCD software*; Nonius BV: Delft, The Netherlands, 1998.
(14) Blessing, R. H. *Acta Crystallogr*. **1995**, *A51*, 33−38.
(15) Sheldrick, G. M. *Programs for Crystal Structure Analysis*, release 97-2; Institüt für Anorganische Chemie der Universität: Göttingen, Germany, 1998.

Table 3. Main Interatomic Distances (Å) in $Mn_{\sim 2.4}Mo_6O_9$

Mn1−O1 (×2)	2.311(4)	Mn3−O7 (×2)	2.308(4)
Mn1−O4	2.770(5)	Mn3−O9 (×2)	2.150(5)
Mn1−O5 (×2)	2.338(4)	Mn4−O2	2.129(6)
Mn1−O9 (×2)	2.129(5)	Mn4−O8	2.069(6)
Mn2−O1 (×2)	2.550(6)	Mn4−O9 (×2)	2.006(5)
Mn2−O6	2.148(6)	Mn5−O2 (×2)	2.176(4)
Mn2−O7 (×2)	2.580(6)	Mn5−O3	2.941(5)
Mn2−O9 (×2)	2.063(6)	Mn5−O5	2.975(5)
Mn3−O3 (×2)	2.335(4)	Mn5−O8 (×2)	2.205(4)
Mn3−O4	2.590(5)	Mn5−O9	2.047(7)
Mo1−Mo1 (×2)	2.8273(2)	Mo4−Mo4 (×2)	2.8273(2)
Mo1−Mo2	2.7702(6)	Mo4−Mo5 (×2)	2.8275(6)
Mo1−Mo2 (×2)	2.8108(6)	Mo4−Mo5	2.8321(6)
Mo1−Mo3 (×2)	2.7868(6)	Mo4−Mo6 (×2)	2.7885(6)
Mo2−Mo1	2.7702(6)	Mo5−Mo4 (×2)	2.8275(6)
Mo2−Mo1 (×2)	2.8108(6)	Mo5−Mo4	2.8321(6)
Mo2−Mo2 (×2)	2.8273(2)	Mo5−Mo5 (×2)	2.8270(8)
Mo2−Mo2 (×2)	2.8652(8)	Mo5−Mo5 (×2)	2.8273(2)
Mo2−Mo3 (×2)	2.8005(6)	Mo5−Mo6 (×2)	2.7718(6)
Mo3−Mo1 (×2)	2.7868(6)	Mo6−Mo4 (×2)	2.7885(6)
Mo3−Mo2 (×2)	2.8005(6)	Mo6−Mo5 (×2)	2.7718(6)
Mo3−Mo3 (×2)	2.8273(2)	Mo6−Mo6 (×2)	2.8273(2)
Mo1−O4 (×2)	2.040(3)	Mo4−O1	2.093(4)
Mo1−O5	2.055(4)	Mo4−O6 (×2)	2.059(3)
Mo1−O7	2.075(4)	Mo4−O8	2.058(4)
Mo2−O2	2.052(4)	Mo5−O3	2.064(4)
Mo2−O5 (×2)	2.081(3)	Mo5−O8 (×2)	2.070(3)
Mo3−O2 (×2)	2.070(3)	Mo6−O1 (×2)	2.089(4)
Mo3−O6	2.101(4)	Mo6−O3 (×2)	2.072(3)
Mo3−O7 (×2)	2.090(4)	Mo6−O4	2.068(4)

20 μA using standard four-probe techniques between 290 and 4.2 K. Ohmic contacts were made by attaching molten indium ultrasonically.

Magnetic Susceptibility Measurements. Susceptibility data were collected on a cold pressed powder sample (ca. 150 mg) in the temperature range between 1.8 and 296 K on an SHE-906 SQUID magnetosusceptometer at applied dc fields ranging from 0.1 to 3 T. The data were subsequently corrected for the diamagnetic contribution of the sample holder.

Results and Discussion

Electron Diffraction Studies. The [100] electron diffraction (ED) pattern (Figure 1) indicates that the reciprocal space of $Mn_{\sim 2.4}Mo_6O_9$ appears as unusual looking at the spot ordering. Reciprocal lattice reconstruction performed in the ED study shows that the intense spots, considered as main reflections, can be indexed in an orthorhombic basic unit cell of parameters $a \sim 16.5$ Å, $b \sim 2.8$ Å, and $c \sim 17.4$ Å. The additional spots, considered as satellite reflections, have, for the most part, incommensurate positions both along b^* and c^*; it should be underlined that some satellite spots belong to [001]* rows in commensurate position along [010]*. To account for the whole satellite reflections, it was necessary to introduce three modulation wave vectors: $q_1^* = 0.28b^*$, $q_2^* = 0.22b^* + 0.48c^*$, and $q_3^* = 0.22b^* - 0.48c^*$. So, this ED pattern suggests strongly the existence of a 3D incommensurate modulation in the crystal. Note that the β and μ components of q_1^* and q_2^* along b^* verify the relation $\beta + \mu = {}^1/_2$ which is not at all imposed by the crystal symmetry. For such a modulation type, whole reflections can be indexed using six integers *hklmnp*;[16] i.e, the diffraction vector can be written as $s^* = ha^* + kb^* + lc^* + mq_1 + nq_2 + pq_3$ where a^*,b^*,c^* are the reciprocal of a,b,c.

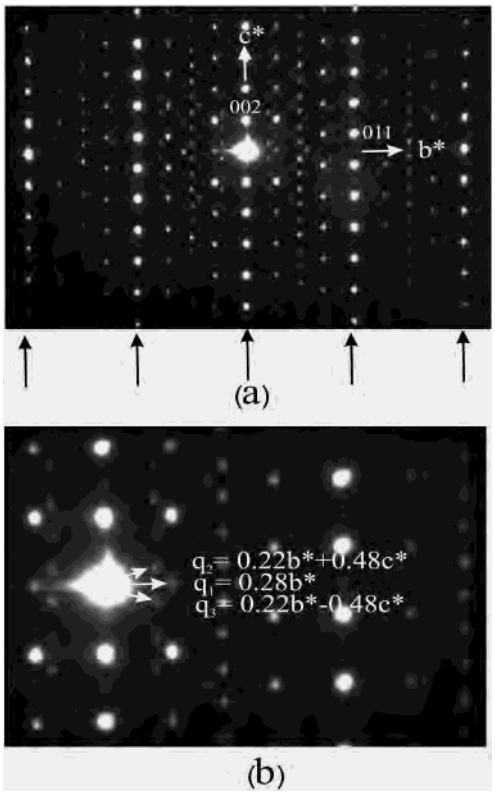

Figure 1. (a) Selected area electron diffraction pattern of $Mn_{\sim 2.4}Mo_6O_9$ along [100]* of the orthorhombic unit cell. Main reflections are indicated by black arrows. (b) Detail showing the three modulation wave vectors (white arrows) used for indexing all spots.

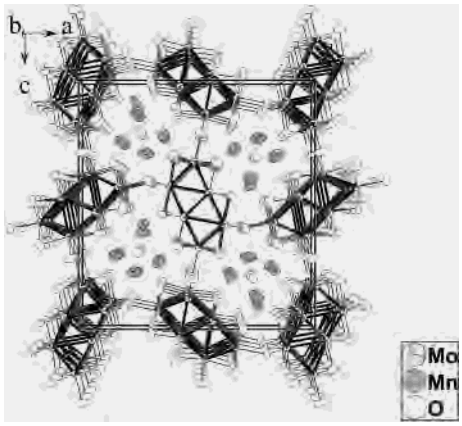

Figure 2. The crystal structure of $Mn_{\sim 2.4}Mo_6O_9$ as viewed down the *b* axis, parallel to the direction of the chain growth. Thick lines denote Mo−Mo bonding, and thin lines, Mo−O bonding. Ellipsoids are drawn at the 97% probability level.

Crystal Structure. To date, only the average crystal structure has been solved. A projected view of the average crystal structure of $Mn_{\sim 2.4}Mo_6O_9$ on the (a,c) plane is shown in Figure 2. It consists of infinite twin chains of edge-sharing Mo_6 octahedra with O atoms above all free edges that are coupled together through interchain Mo−O−Mo linkages to create channels, which are occupied by oxygen and manganese ions.

The twin chain can be seen as resulting from the fusion of two infinite $|Mo_2Mo_{4/2}|_\infty^1$ chains of trans-edge-sharing

(16) Janner, A.; Janssen, T.; de Wolff, P. M. *Acta Crystallogr.* **1983**, *A39*, 658.

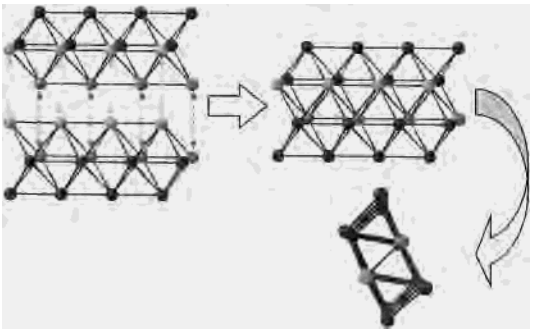

Figure 3. Process of formation of the twin Mo chains.

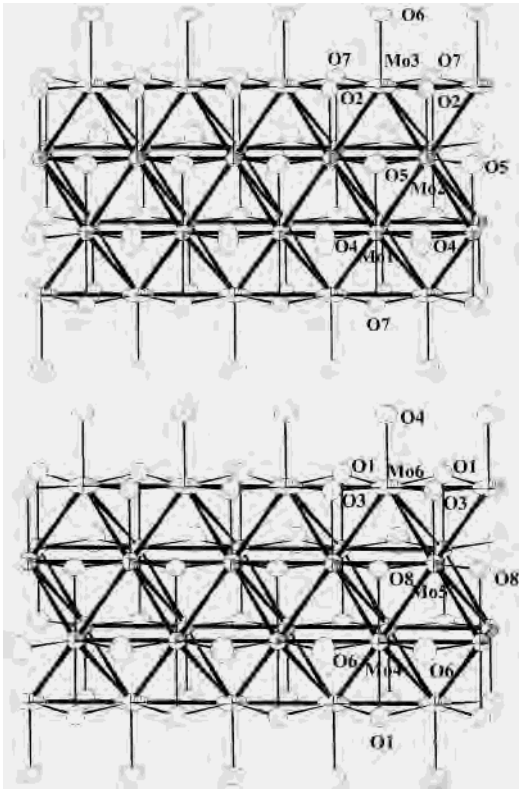

Figure 4. Sections of the two independent molybdenum oxide twin chains with their numbering scheme. Ellipsoids are drawn at the 97% probability level.

octahedra through the sharing of two cis-edges per Mo_6 octahedra (Figure 3). A fragment of a twin chain is represented in Figure 4 with its oxygen environment. Thus, each Mo_6 octahedron has four edges in common with adjacent ones. Although the twin chains appear regular in the average structure, the value of the *U* terms of the atomic displacement parameters of the apical Mo atoms, four times larger than that observed for the other Mo atoms, suggests clearly that in the modulated structure a pairing between the apical Mo atoms, which would lead to a pattern of alternating short and long distances between these atoms, should exist. Except the Mo atoms that are common to the two elementary chains and are linked to three O atoms, the other Mo atoms are surrounded by four and five O atoms as observed in the single chain. The twin chains are then interconnected through O atoms as in $NaMo_4O_6$.[5] The metal−metal and metal−oxygen distances lie between 2.7718(5) and 2.8652(8) and 2.040(3) and 2.101 (4) Å, respectively. Chains of related

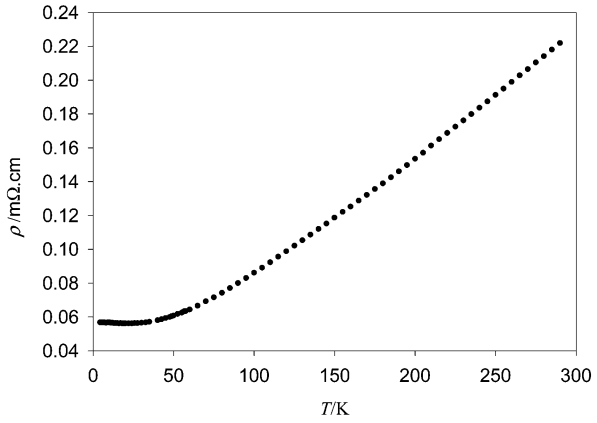

Figure 5. Temperature dependence of the electrical resistivity for $Mn_{\sim 2.4}Mo_6O_9$.

construction have been found in some metal-rich halides of rare earths in which the halogen atoms cap the R_6 octahedra above edges such as $Gd_6I_7C_2$,[17] $Sc_7Cl_{10}C_2$,[18] and Gd_3I_3C.[19] The principal difference between the latter compounds and $Mn_{\sim 2.4}Mo_6O_9$ is the presence of the interstitial carbide anion within the R_6 octahedra that is necessary to stabilize them because of the valence electron deficiency of the chains formed from rare earth metals. In our case, the electron deficiency is compensated by the electron transfer from the cations toward the twin chains. Another great difference resides in the number of electrons available for metal−metal bonding which is only 2 or 3 per formula unit in the metal-rich halides of rare earths, and thus very low compared to the 22.8 electrons in $Mn_{\sim 2.4}Mo_6O_9$.

The large cavities between the oxygen molybdenum chains are occupied by manganese ions distributed on five sites with occupancies less than one within the average structural model. The *U* terms show also abnormally high values; these characteristics lead us to assume the existence of occupancy and displacive modulations for the manganese in the actual crystal, the others atoms, Mo and O, being also concerned by the displacive modulation as discussed previously. Three types of environment are observed for Mn in the average structure with coordination numbers in oxygen atoms of 4, 5, and 7. The 4-coordination polyhedron corresponds to a distorted tetrahedron with the Mn−O distances ranging from 2.006(5) to 2.129(6) Å. The 5-coordination may be described as a square based pyramidal with Mn−O distances in the range 2.047(7)−2.205(4) Å, and the 7-coordination as a monocapped trigonal prism with Mn−O distances in the range 2.063(6)−2.770(5) Å.

Electrical Properties. Four-probe single-crystal resistivity measurements along the needle axis show that $Mn_{\sim 2.4}Mo_6O_9$ exhibits metallic behavior between 4.2 and 300 K with a room resistivity of 0.2 mΩ·cm (Figure 5).

Magnetic Properties. Magnetic susceptibility data for $Mn_{\sim 2.4}Mo_6O_9$ were collected on a powder sample over the temperature range 2−300 K at an applied dc field of 0.5 T.

(17) Simon, A.; Warkentin, E. *Z. Anorg. Allg. Chem.* **1983**, *497*, 79−92.
(18) Kauzlarich, S. M.; Hughbanks, T.; Corbett, J. D.; Klavins, P.; Shelton, R. N. *Inorg. Chem.* **1988**, *27*, 1791−1797.
(19) Mattausch, Hj.; Schwarz, C.; Simon, A. *Z. Kristallogr.* **1987**, *178*, 156−159.

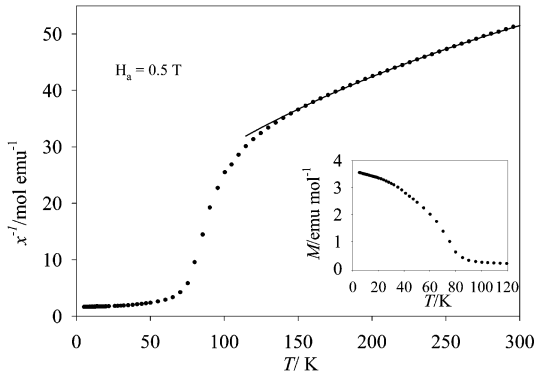

Figure 6. Temperature dependence of the inverse of the molar magnetic susceptibility of $Mn_{\sim 2.4}Mo_6O_9$. The insert shows the temperature dependence of the molar magnetic susceptibility.

The inverse molar magnetic susceptibility as a function of temperature is shown in Figure 6. $Mn_{\sim 2.4}Mo_6O_9$ has paramagnetic behavior above 150 K. Data were fit to a modified Curie−Weiss equation $\chi = C/(T - \theta) + \chi_o$ with $C = 9.69$ emu·K·mol^{-1}, $\theta = -349.0$ K, and $\chi_o = 9.67 \times 10^{-4}$ emu/mol in the temperature range 160−296 K. The magnetic moment derived from this treatment is 5.68 μ_B per manganese ion, which compares favorably with the moment of 5.92 μ_B calculated for high spin Mn(II). This is also in agreement with the calculations of the bond orders s^* [20] for each Mn−O distance, which have allowed us to determine an average valence of 2.01 for the manganese ions.

Below 150 K, $Mn_{\sim 2.4}Mo_6O_9$ behaves like a weak ferromagnet, and the magnetization data indicate a Curie point close to 80 K (insert of Figure 6). Studies of the field dependence of the magnetization at 5 K indicate a remnant magnetization of 3.45×10^{-2} μ_B/Mn^{2+} (Figure 7).

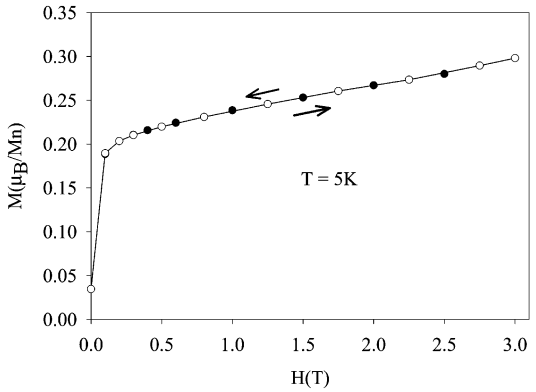

Figure 7. Field dependence of magnetization for $Mn_{\sim 2.4}Mo_6O_9$ at 5 K (● increasing field, ○ decreasing field).

In conclusion, we have prepared a new reduced molybdenum oxide $Mn_{\sim 2.4}Mo_6O_9$ and characterized its electrical and magnetic properties. Electron diffraction studies indicated a complex crystal structure with a 3d incommensurate modulation. The average structure was determined in the space group *Pnma*. The interest in this compound resides in the presence of empty twin chains of trans-edge-sharing Mo_6 octahedra for the first time in a cluster compound. This opens a route to the discovery of a Mo network involving the coupling of three or more parallel chains of trans-edge-sharing Mo_6 octahedra.

Supporting Information Available: X-ray crystallographic file for the $Mn_{\sim 2.4}Mo_6O_9$ compound, in CIF format. This material is available free of charge via the Internet at http://pubs.acs.org.

IC0260365

(20) Brown, I. D.; Wu, K. K. *Acta Crystallogr.* **1976**, *B32*, 1957.